Identification of domains in *Plasmodium falciparum* proteins of unknown function using DALI search on Alphafold predictions

Hannah Michaela Behrens[1,§], Tobias Spielmann[1,#]

[1] Bernhard Nocht Institute for Tropical Medicine, 20359 Hamburg, Germany

[§] Corresponding author: hannah.behrens@bnitm.de

[#] Corresponding author: spielmann@bnitm.de

Abstract

Plasmodium falciparum, the causative agent of malaria, poses a significant global health challenge, yet much of its biology remains elusive. A third of the genes in the *P. falciparum* genome lack annotations regarding their function, impeding our understanding of the parasite's biology. In this study, we employed structure predictions and the DALI search algorithm to analyse proteins encoded by uncharacterized genes in the reference strain 3D7 of *P. falciparum*.

By comparing Alphafold predictions to experimentally determined protein structures in the Protein Data Bank, we found similarities to known domains in 353 proteins of unknown function, shedding light on their potential functions. The lowest-scoring 5% of similarities were additionally validated using the size-independent TM-align algorithm, confirming the detected similarities in 88% of the cases. Notably, in over 70 *P. falciparum* proteins the presence of domains resembling heptatricopeptide repeats, which are typically involvement in RNA binding and processing, was detected. This suggests this family, which is important in transcription in mitochondria and apicoplasts, is much larger in *Plasmodium* parasites than previously thought. The results of this domain search provide a resource to the malaria research community that is expected to inform and enable experimental studies.

Introduction

Plasmodium falciparum, the malaria parasite responsible for over 600 000 deaths every year (World Health Organization, 2022), has a complex life cycle and its biology is still only partly understood. Of its 5268 predicted genes, 1407 remain without any annotation (release 62, January 2023 (Amos et al., 2022; Aurrecoechea et al., 2009)). Annotations of genes are most often based on sequence similarity to well characterized proteins in other organisms (Böhme et al., 2019). As part of an experimental gene-by-gene analysis of unknown proteins encoded on *P. falciparum* chromosome 3 we found that structural similarities of Alphafold structures matched well the experimental evidence of several proteins of unknown function (Kimmel et al., 2023). This indicates that many parasite proteins have a conserved evolutionary origin but evolved beyond recognition on the primary sequence level but not on the structural level. It can therefore be assumed that comparisons of the structural prediction of unknown proteins will yield useful information on proteins currently annotated as unknown. The availability of Alphafold structure predictions (Jumper et al., 2021) now enables the identification of domains based on geometric comparisons, independent of DNA and amino acid sequences. These similarities could provide information about gene products that so far lacked annotation. Here we apply this approach to all genes of unknown function in *P. falciparum*, specifically to the reference strain 3D7. Several sequence-independent algorithms exist to compare protein structures to each other based on geometry, including VAST (Gibrat et al., 1996), Dali (Holm, 2022), Foldseek (van Kempen et al., 2022), CE (Shindyalov & Bourne, 1998), the protein size-

independent scoring algorithm TM-align (Zhang, 2005) and others (reviewed in (Kufareva & Abagyan, 2011)). For this screen we chose the DALI search algorithm as it has several advantages. It is set up to search the PDB and has an integrated graphical user (GUI) interface that also allows quick assessment of PFAM-annotated domains in the aligned structures. Further it has a built-in GUI for visual 3D-assessment of the alignment of hits to the query. We chose an open approach, where we screen all proteins of unknown function for the presence of any domains, rather than searching for a predefined set of domains or restricting the search to a small set of proteins of interest. This has the advantage that discoveries can be made independent of hypotheses that are related to specific processes in the parasite.

Using this approach, we here report the identification of domains with similarities to experimentally determined protein domains in 287 proteins encoded by genes of unknown function from *P. falciparum* 3D7 by an open-ended search. In addition, we used a targeted approach to search for proteins with similarity to the armadillo domain-contain ASA2 and ASA3 proteins which came to our attention as a frequent similarity in the open-ended approach. In this targeted search we found folds resembling heptatricopeptide repeats, which are typically involved in RNA-binding and -processing, in 53 previously un-annotated proteins, indicating that this family is much larger than previously though. We provide these results as a resource to the community to support experimental work.

Results

Identification of domains in proteins of unknown function by open-ended domain search

In order to identify known domains in *P. falciparum* proteins of unknown function, all 1407 proteins which were named protein of unknown function on PlasmoDB (The Plasmodium Genome Database Collaborative, 2001) were selected for analysis. The Alphafold predictions of the proteins encoded by these genes were compared to experimentally determined structures in the protein data bank (PDB) (Burley et al., 2019) using the search algorithm DALI (Holm, 2022). Included in the search were proteins that contained "globular" folds, thus excluding 476 structures which contained solely disordered, extended and fibrous folds, as this is a requirement for successful DALI searches. The resulting 931 hits were visually assessed to exclude structures that aligned only by two or fewer helices or beta strands and this resulted in the identification of similarity to at least one annotated domain in 287 of the 1407 unknown proteins (Figure 1A, Supplementary data 1).

The DALI search assigns a Z-score to each alignment which reflects its quality, where Z-scores of below 2 indicate non-specific similarity. While all except one of the 287 structure alignments that were considered specific and a good fit by the visual inspection had Z- scores of 5 or higher, PF3D7_1336600 had a lower Z-score. However, the lower score in that case was due to its small size as it still showed a very good alignment (also shown in Figure 2). The six highest-scoring similarities had Z-scores of over 30 (Figure 1B). Of the proteins in which domains were identified, 254 contained one newly identified domain, 23 contained two and five proteins contained 3 newly identified domains (Figure 1C). As an example of a protein in which similarity to two domains was detected PF3D7_1013300 was visualized (Figure S1). Among the identified domains, most (>200) domains occurred only once, 27 occurred twice and 17 occurred three times or more (Figure 1D).

To validate these results, the lowest-scoring 5% of similarities found (based on DALI Z-score), were assessed using a second algorithm. For this TM-align was used which is independent of protein size (Zhang, 2005). This algorithm scores similarities between two protein structures on a scale from 0 to

1, where scores over 0.5 indicate that searched structures contain the queried fold. Of the 16 structures assessed 14 showed a TM-score over 0.5 (Figure 2), when compared to the top annotated hit from the DALI search (which was an experimentally determined structure downloaded from the PDB and cropped to the domain that showed similarity). The remaining two showed TM-scores over 0.4. Thus, the two algorithms show good agreement even among the lowest-scored similarities, suggesting a low proportion of false positive similarities.

Comparison with published data

To assess whether the observed similarities have the potential to predict the function of the *P. falciparum* proteins of unknown function, we assess the literature for published experimental data. Although all of the 287 proteins for which similarity was found are encoded by genes that are annotated as of unknown function, some experimental data exists for eight of them (Table 1). The cellular location of the proteins encoded by PF3D7_0307600, PF3D7_0313400 and PF3D7_0319900 was previously assessed by fusing the endogenous gene with the sequence encoding GFP in an experimental screen of genes of unknown function from chromosome three in *P. falciparum* 3D7 parasites (Kimmel et al., 2023) (Table 1). PF3D7_0205600, PF3D7_1013300 and PF3D7_1329500 were analysed by the same approach (Schmidt et al., 2022) (Birnbaum et al., 2017; Khosh-Naucke et al., 2018) while the *P. berghei* ortholog of PF3D7_1132400 was expressed as an endogenous HA-fusion (Zuegge et al., 2001) and their cellular locations observed (Table 1). For PF3D7_0903600 functional data of the orthologue in *Toxoplasma gondii* recently became available (Dubois et al., 2023).

PF3D7_0205600 and PF3D7_1329500 are located in the nucleus, supporting that the identified regions with similarity to CDC45-like and TIG domains, which are found in DNA replication proteins and transcription factors, respectively, might serve the same functions. PF3D7_1013300 showed similarity to both domains that make up nicastrins (Xie et al., 2014)and equally has a transmembrane domain and a short C-terminal tail (Figure S1). In other organisms nicastrin is part of the gamma secretase protein complex that proteolytically processes integral membrane proteins (Shah et al., 2005). Because inhibitors against the human gamma secretase complex had no effect on *P. falciparum* (Li et al., 2009) and homologs of the complex components were not found by sequence similarity, the gamma secretase complex was thought to be absent in *Plasmodium* parasites. Yet, the location of PF3D7_1013300 in the ER and the cell periphery would be consistent with nicastrin in other systems where it gets modified in the Golgi before transport to its final destination at the plasma membrane. Thus, the experimental data is compatible with the observed structural similarity and suggests that at least the nicastrin component of the gamma secretase complex is present in *P. falciparum* parasites.

For PF3D7_0903600 a HOOK_N domain-like fold was detected, which typically occurs in dynein-associated cargo adaptors. It's ortholog in *Toxoplasma gondii* has recently been shown to interact with typical hook-interacting proteins and be involved in processes typical for hook proteins (Dubois et al., 2023), giving credibility to the detected domain.

For PF3D7_0313400 (AAA domain), PF3D7_0319900 (UTRA domain) and PF3D7_1132400 (CRT-like domain) the identified domains are not specific to distinct cellular locations but the experimentally observed cellular location do not disagree with their potential function. As such the domain predictions are possible based on the available experimental data. Solely for PF3D7_0307600, which

138 we found to harbour similarity to a Rad51 domain (typically involved in DNA repair), the GFP-fusion
139 protein was - contrary to our prediction - not found in the nucleus (Kimmel et al., 2023). This might
140 be due to a faulty prediction, a repurposing in *P. falciparum* or an altered cellular location due to the
141 GFP-fusion, which is possible given it is not essential (Kimmel et al., 2023; Schwach et al., 2015).
142
143 **Table 1: Comparison of published data with predicted domains.**

PlasmoDB ID	Newly identified domain and its function	Experimental data available for protein	Match of domain identification and experimental data
PF3D7_0205600	CDC45-like; DNA replication (Z-score 28.0)	GFP-fusion localizes to nucleus and cytoplasm (Birnbaum et al., 2017).	Predicted function **supported** by experimental data.
PF3D7_0307600	Rad51; DNA repair (Z-score 24.2)	GFP-fusion gives unknown localization pattern within the parasite (Kimmel et al., 2023).	Predicted function **not supported** by experimental data. Expected would be nuclear localization.
PF3D7_0313400	AAA; chaperone (Z-score 13.5)	GFP-fusion localizes to the parasite cytoplasm (Kimmel et al., 2023).	Predicted function **possible** based on experimental data.
PF3D7_0319900	UTRA; Ligand-binding, modulates transcription factor activity in response to small molecules (Z-score 6.7)	GFP-fusion gives unknown localization pattern in the parasite (Kimmel et al., 2023).	Predicted function **possible** based on experimental data.
PF3D7_0903600	HOOK_N; dynein-associated cargo adaptor proteins (Z-score 12.0)	*Toxoplasma gondii* homolog *Tg*HOOK regulates apical positioning and secretion of micronemes and contributes to egress, motility, host cell attachment, and invasion. Interacts with homologs of HOOK interaction partners TgFTS or TgHIP. (Dubois et al., 2023).	Predicted function **supported** by experimental data.
PF3D7_1013300	Ncstrn_small (small lobe) and Nicastrin (large lobe); Two domains making up nicastrin, a part of complex for intra-membrane proteolysis of integral membrane proteins. This protein is modified in Golgi or trans-Golgi network. (Z-score 20.4)	GFP-fusion localizes to the periphery of ring stages, trophozoites and schizonts and is visible in ER in trophozoites and schizonts. (Khosh-Naucke et al., 2018). Isolated from detergent-resistant membranes. HA-fusion gives "dotted labelling within the parasite cytoplasm" (Yam et al., 2013).	Predicted function **supported** by experimental data.
PF3D7_1132400	CRT-like; chloroquine resistance transporter and homologues. Arabidopsis homologues involved in thiol transport from plastid to cytosol. (Z-score 33.8)	In *P. berghei* non-nuclear, non-apicoplast signal of HA-fusion protein. Predicted to have 9 to 10 TM domains. Western blot shows electrophoresis anomalies common to membrane proteins (Sayers et al., 2018).	Predicted function **possible** based on experimental data.
PF3D7_1329500	TIG; in cell surface receptors and in transcription factors for DNA binding (Z-score 8.1)	GFP-fusion localizes to nucleus in ring and trophozoite stage, in addition foci in the parasite periphery at K13 compartment in trophozoites stage (Schmidt et al., 2022).	Predicted function **supported** by experimental data.

144

145 **Proteins containing Armadillo-like domains**
146 It stood out that many unknown *P. falciparum* proteins showed similarity to Mitochondrial ATP
147 synthase subunit ASA2 and Mitochondrial F1F0 ATP synthase associated 32 kDa protein ASA3. These
148 two proteins are part of the Polytomella F-ATP synthase complex for which structures of several
149 states were determined by single-particle cryo-electron microscopy (Murphy et al., 2019). As
150 according to Interpro no domains are annotated in the ASA2 and ASA3 proteins, no equivalent
151 domains in the structurally similar *P. falciparum* proteins could be annotated by our approach. To
152 annotate this large group of *P. falciparum* proteins, we therefore sought to identify the shared
153 domain of ASA2 and ASA3. Using their structures from PDB (PDB 6rd4), we performed a DALI search
154 against all PDB structures. The top hits for either protein were ASA2 and ASA3, suggesting that both
155 were very similar to each other. Further both were similar to proteins containing armadillo domains
156 (PF00514), for example in catenin delta (PDB 3L6X (Ishiyama et al., 2010)), plakoglobin (PDB 3IFQ
157 (Choi et al., 2009)), plakophilin (PDB 1XM9 (Choi & Weis, 2005)) and several other proteins,
158 suggesting that both ASA2 and ASA3 contain domains, which are made up of several armadillo
159 repeats.
160
161 We then performed DALI searches of these armadillo domains from ASA2 (residues 1-326) and ASA3
162 (full length) against all Alphafold-predicted structures of *P. falciparum* in the database. 1158 genes
163 were found to encode proteins that contains domains similar to ASA2, ASA3 or both. As the Z-score is
164 dependent on protein size, a suitable cut-off had to be determined for the common domain of ASA2
165 and ASA3. Spot checks of hits across different Z-scores were performed and showed that hits with a
166 Z-score of 6.5 or higher showed good similarity to ASA2 or ASA3, with alignment of more than three
167 armadillo repeats which each consist of one helix pair. To avoid false positives, an even more
168 stringent Z-score cut-off of 7.0 was chosen which resulted in 121 *P. falciparum* (in 3D7) protein hits
169 (Figure 3A, Supplementary data 2). All of them were found in both searches (ASA2 and ASA3). The
170 hits included 18 heptatricopeptide repeat proteins, 13 RAP (**R**NA-binding domain abundant in
171 **Api**complexans) proteins - both families are thought to be RNA-binding (Hillebrand et al., 2018; Hollin
172 et al., 2021), - 3 that contain heptatricopeptide repeats and a RAP domain, 3 proteins that are named
173 armadillo-domain containing proteins, 72 proteins of unknown function and 12 proteins with other
174 annotations (Figure 3B). In 6 of these, there were also new domains identified in the open-ended
175 DALI search shown in Figure 1, including DUF559, Importin-beta, Exportin 1-like, Armadillo domain
176 and Atypical Armadillo domain. Both DUF559 domains (in PF3D7_0104600 and PF3D7_1207900) did
177 not overlap with the identified armadillo domain, while the remaining four covered the same
178 residues for which similarity to the ASA2-ASA3-armadillo domain was found (Figure S2).
179
180 The amino acid sequences of these 121 proteins were aligned using Clustal Omega (Sievers & Higgins,
181 2018). The sequences of the proteins with annotation did not cluster according to their PlasmoDB
182 annotations and generally showed little amino acid sequence similarity. We therefore decided to
183 cluster them by structure. However, the 121 *P. falciparum* hits with similarity to ASA2 and ASA3 were
184 too many to do this in one batch, thus first the Alphafold predictions of only those with an
185 annotation in PlasmoDB were clustered using the DALI all-against-all algorithm. Two distinct clusters
186 were observed and named cluster 1 and cluster 2 (Figure 3C). Cluster 1 was found to contain all
187 heptatricopeptide repeat proteins, all RAP proteins and ARM2 (Figure 2C-F). All of these proteins are
188 known or predicted to be RNA-binding proteins (Hillebrand et al., 2018; Hollin et al., 2021; Tang et
189 al., 2019), while all proteins in cluster 2 are protein-binding proteins, some of which can also bind
190 RNA (Frankel & Knoll, 2009; Fritz et al., 2009; Geiger et al., 2020; Henrici et al., 2020; Jacot et al.,

191 2016; Jakel, 1998; Kumar et al., 2023; Xu et al., 2002). Three structures were randomly chosen to
192 represent each cluster (Figure 3C-E) and aligned to batches of the 72 unknown *P. falciparum* proteins
193 that harboured similarity to ASA2 and ASA3 (Figure S3). This assigned 53 new proteins to cluster 1
194 and one new protein to cluster 2, while 18 proteins could not be assigned to either cluster (Figure
195 3F).
196
197 Of the 20 proteins previously known to contain RAP domains, 5 were known to also contain
198 heptatricopeptide repeats. Of the remaining 15 RAP proteins, 13 showed up in our search, suggesting
199 that these also contain heptatricopeptide repeats. The DUF559 domains identified in two newly
200 identified heptatricopeptide repeat-like proteins also show some similarity to RAP domains. Thus,
201 the co-occurrence of RAP domains with heptatricopeptide repeats in the same protein seems to be a
202 common combination.
203
204 **Discussion**
205 In this study we used the DALI algorithm to search for similarities of the available Alphafold-predicted
206 structures of all unknown *P. falciparum* (3D7) proteins to known domains in experimentally
207 determined structures. This similarity search reduced the number of proteins without any annotation
208 from 1407 to 1054, which is a 25% reduction. We expect the resulting set of several hundred
209 identified domains to be a useful resource to the malaria research community that will help
210 streamline further annotation and characterization efforts, and expected to aid the understanding of
211 the molecular mechanisms of malaria parasites. It provides information on the potential function of
212 these *P. falciparum* protein inferred from the structural similarity to known proteins in other
213 organisms. Additionally, in combination with functional and interactome data these domain searches
214 can aid and substantiate the assignment of proteins to protein groups or complexes which together
215 serve a specific function as e.g. recently done for proteins in mitosis (Kimmel et al., 2023, Brusini et
216 al., 2022).
217
218 Open-ended approaches have the advantage that they can discover unexpected components and
219 pathways. The search in this study gives hints to the unexpected presence of nicastrin, which is part
220 of a functionality thought to be absent in *Plasmodium* parasites. This approach can also provide hints
221 for proteins that were expected to be present but had so far not been identified. One example from
222 our dataset is PF3D7_0404300 which shows similarity to Ran-binding proteins and could be a missing
223 component in transport in and out of the nucleus.
224
225 Unexpectedly, we discovered a large group of proteins in the parasite with very similar domains,
226 including all known heptatricopeptide repeat and RAP proteins as well as 53 unknown proteins.
227 Proteins containing heptatricopeptide repeats are known to bind and process polycistronic precursor
228 RNAs into mRNAs and rRNAs for the mitochondrial ribosomes and to stabilize mRNAs to prevent
229 decay (Hillebrand et al., 2018). Heptatricopeptide repeats proteins contain 37 amino acid long
230 repeats, while proteins from the related families of pentatricopepide repeat proteins and
231 octatricopeptide repeats proteins contain repeats which are 35 and 38 amino acids in length. Hepta-,
232 penta- and octatricopeptide repeat proteins perform comparable RNA binding and processing
233 functions, yet their distribution among different organism groups, like plants, apicomplexans and
234 animals, varies (Hillebrand et al., 2018). In humans only 6 heptatricopeptide repeat proteins have
235 been detected while around 70 were predicted in plants and dinoflagellates. In plants this is in
236 addition to 450 pentatricopepide repeat proteins. In addition to the 18 previously described

heptatricopeptide repeat proteins in *Plasmodium*, we here identified many more potential members of this group. If all 54 unknown proteins in cluster 1 of our clustering of the ASA2 and ASA3 hits indeed are such RNA-binding proteins, this would place the number of heptatricopeptide repeat-like RNA-binding proteins in *Plasmodium* (72) in a similar range as in plants. Interestingly, while some the *P. falciparum* proteins with similarity to heptatricopeptide repeat proteins contain insertions that break the 37-amino acid repeat motif that gives this domain its name, the geometry of the 37-amino acid repeat seems conserved.

Another interesting aspect is that we found heptatricopeptide repeat-like folds in a large proportion of proteins containing RAP and RAP-like DUF559 domains. RAP domains consist of a restriction endonuclease-like fold and are found in RNA-binding proteins (Hollin et al., 2021). Thus, heptatricopeptide repeats and RAP domains seem to be a common combination, suggesting that the two domains might act in concert.

While we believe this search to provide a valuable and useful resource, there are a number of limitations. The first inherent limitation is that this study used predicted structures of *P. falciparum* proteins rather than experimentally determined structures, which should not be viewed with the same confidence as experimentally determined structures. This circumstance has been discussed extensively following the introduction of Alphafold (Jones & Thornton, 2022; Subramaniam & Kleywegt, 2022; Terwilliger et al., 2022).

A second limitation was that the search presented here was not exhaustive. To the predicted structures, we applied DALI, the only search platform with which it was feasible to manually analyse several hundred protein structures in a reasonable time. This throughput is largely possible because of the built-in alignment and domain annotation viewers. The DALI algorithm scores search results based on length and quality of the structure alignment of the whole query structure.
As a result, this algorithm favoured the discovery of one domain of highest confidence, while further domains in the same protein were only discovered if they incidentally had similar scores as the first domain or if they occurred in the same experimentally determined structure that the query aligned to. This is one reason, why the search presented in this study was not exhaustive. Other search algorithms could circumvent this drawback, for example the VAST algorithm first detects potential domains in the query structure and then performs searches for each of them individually in addition to the search with the complete query structure. Generally, the use of other search algorithms, such as VAST (Gibrat et al., 1996), Foldseek (van Kempen et al., 2022) and PDBeFold (Krissinel & Henrick, 2004), might result in the discovery of different domain similarities due to their different implementations and ways of scoring similarity. This search being not exhaustive is an important limitation that should be kept in mind when using these findings. Nevertheless, some of the identified domains already give clear functional indications and a protein of interest can then be analysed in more detail using other algorithms in which case further domains might be identified.

A third limitation of our approach is that domains that were not annotated in experimentally determined structures could not be found. Searching against predicted structures of well-studied and annotated proteins might therefore expand the number of detected domains. Of course, with the caveat that predicted structures harbour some uncertainty.

282 Finally, the identified domains were not all computationally and none were experimentally validated
283 in this study. Computational validation could be achieved by re-assessing the detected similarities
284 using a second algorithm. This could for instance be the cealign command in Pymol (Figure 1B)
285 followed by confirming or rejecting annotations based on a cut-off score, as we have done previously
286 (Schmidt et al., 2022). It could also be done with the TM-align algorithm which has a pre-defined cut-
287 off (Zhang, 2005) and was here used to validate the lowest 5% of the hits from this work. This
288 confirmed 14 of 16 hits, overall giving a good credibility for the detected similarities, particularly as it
289 can be assumed that the hits with higher scores are more reliable. Experimental validation is the gold
290 standard for any structure prediction (Sanderson & Rayner, 2017). The assessment of available data
291 in published literature on eight proteins annotated here, suggests that the majority of similarities
292 found might align with the function that can be inferred from the domain similarities. However, a
293 case-by-case validation is the only way to know whether the domains were identified correctly and
294 whether these domains serve the same function in *P. falciparum* as in other organisms. We did not
295 embark on a systematic experimental validation as this would take a considerable amount of time
296 and we believe that rapidly providing these search results to the wider community will be more
297 beneficial.
298
299 In conclusion, the results presented here are an example for the power of sequence-independent
300 structure comparison approaches for reducing the number of genes lacking annotation and
301 information on their potential biological function. Here applied to *P. falciparum*, it sheds light on the
302 biology of the malaria parasite and provides starting points for future research which will lead to a
303 better understanding of the biology of this pathogen.
304
305
306 **Methods**
307
308 **Open-ended search**
309 Lists of genes were downloaded from PlasmoDB v61 based on genomic location. All genes which
310 contained the word "unknown" in the gene name, for example "conserved Plasmodium protein,
311 unknown function", were included in the analysis. Pseudogenes were excluded.
312 Available Alphafold (alphafold.ebi.ac.uk, accessed December 2022-Mai 2023) (Jumper et al., 2021)
313 structures were visually assessed for a globular and compact fold which is a prerequisite for a
314 successful DALI search (Holm, 2022). The suitable Alphafold structures were submitted to a DALI PDB
315 search as available in the web application (http://ekhidna2.biocenter.helsinki.fi/dali/, accessed
316 December 2022-Mai 2023). The matches against PDB90 were analysed. The hits with the highest Z-
317 scores were visually assessed for suitable alignment (excluded alignment of just 2 or fewer α-helices
318 or β-strands) in the DALI 3D visualization tool. Of the top seven to ten hits with good alignment, the
319 Pfam 35.0 (Mistry et al., 2021) domain annotations were viewed in the DALI PFAM tool. A domain
320 annotation for a region of a PDB hit that aligned to the query Alphafold structure was considered a
321 reliable hit if there were no conflicting domain annotation. Domain annotations were considered
322 conflicting if other proteins with differently annotated domains aligned to the same amino acid
323 residues and had a Z-score within 1.0 of the protein harbouring the domain of interest.
324
325 **Validation with TM-align**
326 The 5% of domains with the lowest Z-score resulting from the open-ended DALI search were further
327 validated. For each of these, the PDB structure of the top hit of the DALI search was cropped to only

contain the residues annotated as the domain for which similarity was found. Where the top hit did not contain this annotation, the highest-scoring PDB structure with this annotation was used. The Alphafold structure was compared with this cropped PDB structure using TM-align (Zhang, 2005) as available in the web application (https://seq2fun.dcmb.med.umich.edu//TM-align/, accessed December 2022-Mai 2023). The TM-score based on the length of the cropped PDB structure was assessed.

ASA2/ASA3 search

All protein structures predicted for *P. falciparum* by AlphaFold (Jumper et al., 2021) were searched using ASA2 residues 1-326 and full length ASA3 (chain 2 and 3 of PDB 6rd4 (Murphy et al., 2019)) using the DALI AF search (Holm, 2022). Alignments were visually assessed for at least 3 aligned armadillo repeats (helix pairs), resulting in all proteins with a Z-score larger or equal to 7.0 to be included for further analysis.

Visualization and further assessment

Protein structures were analysed and visualized using PyMol 2.4.0 (Schrödinger, USA). Alignments were performed using the PyMol command cealign. Figures were arranged in CorelDraw X6-8.

Acknowledgements

We thank Jesper Del Messier, Ana Ivan, Jan Stephan Wichers-Misterek and Isabelle Henshall for helpful discussions. This research made use of PlasmoDB, a VEuPathDB resource (Amos et al., 2022). HMB acknowledges funding by the Ortrud Mührer Fellowship of the Vereinigung der Freunde des Tropeninstituts Hamburg e.V.. HMB and TS acknowledge funding by the European Research Council (ERC, grant 101021493).

References

Amos, B., Aurrecoechea, C., Barba, M., Barreto, A., Basenko, E. Y., Bażant, W., Belnap, R., Blevins, A. S., Böhme, U., Brestelli, J., Brunk, B. P., Caddick, M., Callan, D., Campbell, L., Christensen, M. B., Christophides, G. K., Crouch, K., Davis, K., DeBarry, J., … Zheng, J. (2022). VEuPathDB: the eukaryotic pathogen, vector and host bioinformatics resource center. *Nucleic Acids Research*, *50*(D1), D898–D911. https://doi.org/10.1093/nar/gkab929

Aurrecoechea, C., Brestelli, J., Brunk, B. P., Dommer, J., Fischer, S., Gajria, B., Gao, X., Gingle, A., Grant, G., Harb, O. S., Heiges, M., Innamorato, F., Iodice, J., Kissinger, J. C., Kraemer, E., Li, W., Miller, J. A., Nayak, V., Pennington, C., … Wang, H. (2009). PlasmoDB: a functional genomic database for malaria parasites. *Nucleic Acids Research*, *37*(Database), D539–D543. https://doi.org/10.1093/nar/gkn814

Birnbaum, J., Flemming, S., Reichard, N., Soares, A. B., Mesén-ramírez, P., Jonscher, E., Bergmann, B., & Spielmann, T. (2017). A genetic system to study Plasmodium falciparum protein function. *Nature Methods*, *14*(4), 450–456. https://doi.org/10.1038/nmeth.4223

Böhme, U., Otto, T. D., Sanders, M., Newbold, C. I., & Berriman, M. (2019). Progression of the canonical reference malaria parasite genome from 2002–2019. *Wellcome Open Research*, *4*, 58. https://doi.org/10.12688/wellcomeopenres.15194.2

Brusini, L., Dos Santos Pacheco, N., Tromer, E. C., Soldati-Favre, D., & Brochet, M. (2022). Composition and organization of kinetochores show plasticity in apicomplexan chromosome segregation. *J Cell Biol*., *22*(9), e202111084. https://doi.org/10.1083/jcb.202111084

373 Burley, S. K., Berman, H. M., Bhikadiya, C., Bi, C., Chen, L., Costanzo, L. Di, Christie, C., Duarte, J. M.,
374 Dutta, S., Feng, Z., Ghosh, S., Goodsell, D. S., Green, R. K., Guranovic, V., Guzenko, D., Hudson,
375 B. P., Liang, Y., Lowe, R., Peisach, E., … Ioannidis, Y. E. (2019). Protein Data Bank: the single
376 global archive for 3D macromolecular structure data. *Nucleic Acids Research*, *47*(D1), D520–
377 D528. https://doi.org/10.1093/nar/gky949

378 Choi, H.-J., Gross, J. C., Pokutta, S., & Weis, W. I. (2009). Interactions of Plakoglobin and β-Catenin
379 with Desmosomal Cadherins. *Journal of Biological Chemistry*, *284*(46), 31776–31788.
380 https://doi.org/10.1074/jbc.M109.047928

381 Choi, H.-J., & Weis, W. I. (2005). Structure of the Armadillo Repeat Domain of Plakophilin 1. *Journal of*
382 *Molecular Biology*, *346*(1), 367–376. https://doi.org/10.1016/j.jmb.2004.11.048

383 Dubois, D. J., Chehade, S., Marq, J.-B., Venugopal, K., Maco, B., Puig, A. T. I., Soldati-Favre, D., &
384 Marion, S. (2023). *Toxoplasma gondii* HOOK-FTS-HIP Complex is Critical for Secretory Organelle
385 Discharge during Motility, Invasion, and Egress. *MBio*. https://doi.org/10.1128/mbio.00458-23

386 Frankel, M. B., & Knoll, L. J. (2009). The Ins and Outs of Nuclear Trafficking: Unusual Aspects in
387 Apicomplexan Parasites. *DNA and Cell Biology*, *28*(6), 277–284.
388 https://doi.org/10.1089/dna.2009.0853

389 Fritz, J., Strehblow, A., Taschner, A., Schopoff, S., Pasierbek, P., & Jantsch, M. F. (2009). RNA-
390 Regulated Interaction of Transportin-1 and Exportin-5 with the Double-Stranded RNA-Binding
391 Domain Regulates Nucleocytoplasmic Shuttling of ADAR1. *Molecular and Cellular Biology*, *29*(6),
392 1487–1497. https://doi.org/10.1128/MCB.01519-08

393 Geiger, M., Brown, C., Wichers, J. S., Strauss, J., Lill, A., Thuenauer, R., Liffner, B., Wilcke, L., Lemcke,
394 S., Heincke, D., Pazicky, S., Bachmann, A., Löw, C., Wilson, D. W., Filarsky, M., Burda, P.-C.,
395 Zhang, K., Junop, M., & Gilberger, T. W. (2020). Structural Insights Into PfARO and
396 Characterization of its Interaction With PfAIP. *Journal of Molecular Biology*, *432*(4), 878–896.
397 https://doi.org/10.1016/j.jmb.2019.12.024

398 Gibrat, J.-F., Madej, T., & Bryant, S. H. (1996). Surprising similarities in structure comparison. *Current*
399 *Opinion in Structural Biology*, *6*(3), 377–385. https://doi.org/10.1016/S0959-440X(96)80058-3

400 Henrici, R. C., Edwards, R. L., Zoltner, M., van Schalkwyk, D. A., Hart, M. N., Mohring, F., Moon, R. W.,
401 Nofal, S. D., Patel, A., Flueck, C., Baker, D. A., John, A. R. O., Field, M. C., & Sutherland, C. J.
402 (2020). The plasmodium falciparum artemisinin susceptibility-associated ap-2 adaptin μ subunit
403 is clathrin independent and essential for schizont maturation. *MBio*, *11*(1), 1–16.
404 https://doi.org/10.1128/mBio.02918-19

405 Hillebrand, A., Matz, J. M., Almendinger, M., Müller, K., Matuschewski, K., & Schmitz-Linneweber, C.
406 (2018). Identification of clustered organellar short (cos) RNAs and of a conserved family of
407 organellar RNA-binding proteins, the heptatricopeptide repeat proteins, in the malaria parasite.
408 *Nucleic Acids Research*, *46*(19), 10417–10431. https://doi.org/10.1093/nar/gky710

409 Hollin, T., Jaroszewski, L., Stajich, J. E., Godzik, A., & Le Roch, K. G. (2021). Identification and
410 phylogenetic analysis of RNA binding domain abundant in apicomplexans or RAP proteins.
411 *Microbial Genomics*, *7*(3). https://doi.org/10.1099/mgen.0.000541

412 Holm, L. (2022). Dali server: structural unification of protein families. *Nucleic Acids Research*, *50*(W1),
413 W210–W215. https://doi.org/10.1093/nar/gkac387

414 Ishiyama, N., Lee, S.-H., Liu, S., Li, G.-Y., Smith, M. J., Reichardt, L. F., & Ikura, M. (2010). Dynamic and
415 Static Interactions between p120 Catenin and E-Cadherin Regulate the Stability of Cell-Cell
416 Adhesion. *Cell*, *141*(1), 117–128. https://doi.org/10.1016/j.cell.2010.01.017

417 Jacot, D., Tosetti, N., Pires, I., Stock, J., Graindorge, A., Hung, Y.-F., Han, H., Tewari, R., Kursula, I., &
418 Soldati-Favre, D. (2016). An Apicomplexan Actin-Binding Protein Serves as a Connector and Lipid
419 Sensor to Coordinate Motility and Invasion. *Cell Host & Microbe*, *20*(6), 731–743.
420 https://doi.org/10.1016/j.chom.2016.10.020

421 Jakel, S. (1998). Importin beta , transportin, RanBP5 and RanBP7 mediate nuclear import of
422 ribosomal proteins in mammalian cells. *The EMBO Journal*, *17*(15), 4491–4502.
423 https://doi.org/10.1093/emboj/17.15.4491

424 Jones, D. T., & Thornton, J. M. (2022). The impact of AlphaFold2 one year on. *Nature Methods*, *19*(1),
425 15–20. https://doi.org/10.1038/s41592-021-01365-3

426 Jumper, J., Evans, R., Pritzel, A., Green, T., Figurnov, M., Ronneberger, O., Tunyasuvunakool, K.,
427 Bates, R., Žídek, A., Potapenko, A., Bridgland, A., Meyer, C., Kohl, S. A. A., Ballard, A. J., Cowie,
428 A., Romera-Paredes, B., Nikolov, S., Jain, R., Adler, J., … Hassabis, D. (2021). Highly accurate
429 protein structure prediction with AlphaFold. *Nature*, *596*(7873), 583–589.
430 https://doi.org/10.1038/s41586-021-03819-2

431 Khosh-Naucke, M., Becker, J., Mesén-Ramírez, P., Kiani, P., Birnbaum, J., Fröhlke, U., Jonscher, E.,
432 Schlüter, H., & Spielmann, T. (2018). Identification of novel parasitophorous vacuole proteins in
433 P. falciparum parasites using BioID. *International Journal of Medical Microbiology*, *308*(1), 13–
434 24. https://doi.org/10.1016/j.ijmm.2017.07.007

435 Kimmel, J., Schmitt, M., Sinner, A., Jansen, P. W. T. C., Mainye, S., Ramón-Zamorano, G., Toenhake, C.
436 G., Wichers-Misterek, J. S., Cronshagen, J., Sabitzki, R., Mesén-Ramírez, P., Behrens, H. M.,
437 Bártfai, R., & Spielmann, T. (2023). Gene-by-gene screen of the unknown proteins encoded on
438 Plasmodium falciparum chromosome 3. *Cell Systems*, *14*(1), 9-23.e7.
439 https://doi.org/10.1016/j.cels.2022.12.001

440 Krissinel, E., & Henrick, K. (2004). Secondary-structure matching (SSM), a new tool for fast protein
441 structure alignment in three dimensions. *Acta Crystallographica Section D Biological*
442 *Crystallography*, *60*(12), 2256–2268. https://doi.org/10.1107/S0907444904026460

443 Kufareva, I., & Abagyan, R. (2011). *Methods of Protein Structure Comparison* (pp. 231–257).
444 https://doi.org/10.1007/978-1-61779-588-6_10

445 Kumar, A., Vadas, O., Dos Santos Pacheco, N., Zhang, X., Chao, K., Darvill, N., Rasmussen, H. Ø., Xu, Y.,
446 Lin, G. M.-H., Stylianou, F. A., Pedersen, J. S., Rouse, S. L., Morgan, M. L., Soldati-Favre, D., &
447 Matthews, S. (2023). Structural and regulatory insights into the glideosome-associated
448 connector from Toxoplasma gondii. *ELife*, *12*. https://doi.org/10.7554/eLife.86049

449 Li, X., Chen, H., Bahamontes-Rosa, N., Kun, J. F. J., Traore, B., Crompton, P. D., & Chishti, A. H. (2009).
450 Plasmodium falciparum signal peptide peptidase is a promising drug target against blood stage
451 malaria. *Biochemical and Biophysical Research Communications*, *380*(3), 454–459.
452 https://doi.org/10.1016/j.bbrc.2009.01.083

453 Mistry, J., Chuguransky, S., Williams, L., Qureshi, M., Salazar, G. A., Sonnhammer, E. L. L., Tosatto, S.
454 C. E., Paladin, L., Raj, S., Richardson, L. J., Finn, R. D., & Bateman, A. (2021). Pfam: The protein

455 families database in 2021. *Nucleic Acids Research*, *49*(D1), D412–D419.
456 https://doi.org/10.1093/nar/gkaa913

457 Murphy, B. J., Klusch, N., Langer, J., Mills, D. J., Yildiz, Ö., & Kühlbrandt, W. (2019). Rotary substates
458 of mitochondrial ATP synthase reveal the basis of flexible F_1-F_o coupling. *Science*, *364*(6446).
459 https://doi.org/10.1126/science.aaw9128

460 Sanderson, T., & Rayner, J. C. (2017). PhenoPlasm: a database of disruption phenotypes for malaria
461 parasite genes. *Wellcome Open Research*, *2*, 45.
462 https://doi.org/10.12688/wellcomeopenres.11896.2

463 Sayers, C. P., Mollard, V., Buchanan, H. D., McFadden, G. I., & Goodman, C. D. (2018). A genetic
464 screen in rodent malaria parasites identifies five new apicoplast putative membrane
465 transporters, one of which is essential in human malaria parasites. *Cellular Microbiology*, *20*(1).
466 https://doi.org/10.1111/cmi.12789

467 Schmidt, S., Wichers-misterek, J. S., Behrens, H. M., Birnbaum, J., Henshall, I., Jonscher, E., Flemming,
468 S., & Spielmann, T. (2022). The Kelch13 compartment is a hub of highly divergent vesicle
469 trafficking proteins in malaria parasites. *BioRxiv [Preprint]*.
470 https://doi.org/https://doi.org/10.1101/2022.12.15.520209

471 Schwach, F., Bushell, E., Gomes, A. R., Anar, B., Girling, G., Herd, C., Rayner, J. C., & Billker, O. (2015).
472 PlasmoGEM, a database supporting a community resource for large-scale experimental genetics
473 in malaria parasites. *Nucleic Acids Research*, *43*(D1), D1176–D1182.
474 https://doi.org/10.1093/nar/gku1143

475 Shah, S., Lee, S.-F., Tabuchi, K., Hao, Y.-H., Yu, C., LaPlant, Q., Ball, H., Dann, C. E., Südhof, T., & Yu, G.
476 (2005). Nicastrin Functions as a γ-Secretase-Substrate Receptor. *Cell*, *122*(3), 435–447.
477 https://doi.org/10.1016/j.cell.2005.05.022

478 Shindyalov, I. N., & Bourne, P. E. (1998). Protein structure alignment by incremental combinatorial
479 extension (CE) of the optimal path. *Protein Engineering Design and Selection*, *11*(9), 739–747.
480 https://doi.org/10.1093/protein/11.9.739

481 Sievers, F., & Higgins, D. G. (2018). Clustal Omega for making accurate alignments of many protein
482 sequences. *Protein Science*, *27*(1), 135–145. https://doi.org/10.1002/pro.3290

483 Subramaniam, S., & Kleywegt, G. J. (2022). A paradigm shift in structural biology. *Nature Methods*,
484 *19*(1), 20–23. https://doi.org/10.1038/s41592-021-01361-7

485 Tang, Y., Meister, T. R., Walczak, M., Pulkoski-Gross, M. J., Hari, S. B., Sauer, R. T., Amberg-Johnson,
486 K., & Yeh, E. (2019). A mutagenesis screen for essential plastid biogenesis genes in human
487 malaria parasites. *PLOS Biology*, *17*(2), e3000136.
488 https://doi.org/10.1371/journal.pbio.3000136

489 Terwilliger, T., Liebschner, D., Croll, T. I., Williams, C. J., McCoy, A. J., Poon, B. K., Afonine, P. V.,
490 Oeffner, R. D., Richardson, J. S., Read, R. J., & Adams, P. D. (2022). AlphaFold predictions: great
491 hypotheses but no match for experiment. *BioRxiv*. https://doi.org/10.1101/2022.11.21.517405

492 The Plasmodium Genome Database Collaborative. (2001). PlasmoDB: An integrative database of the
493 Plasmodium falciparum genome. Tools for accessing and analyzing finished and unfinished
494 sequence data. *Nucleic Acids Research*, *29*(1), 66–69. https://doi.org/10.1093/nar/29.1.66

van Kempen, M., Kim, S. S., Tumescheit, C., Mirdita, M., Lee, J., Gilchrist, C. L. M., Söding, J., & Steinegger, M. (2022). Fast and accurate protein structure search with Foldseek. *BioRxiv*. https://www.biorxiv.org/content/10.1101/2022.02.07.479398v5

World Health Organization. (2022). *World malaria report 2022*. https://www.who.int/publications/i/item/9789240064898

Xie, T., Yan, C., Zhou, R., Zhao, Y., Sun, L., Yang, G., Lu, P., Ma, D., & Shi, Y. (2014). Crystal structure of the γ-secretase component nicastrin. *Proceedings of the National Academy of Sciences of the United States of America*, *111*(37), 13349–13354. https://doi.org/10.1073/pnas.1414837111

Xu, X., Yamasaki, H., Feng, Z., & Aoki, T. (2002). Molecular cloning and characterization of Plasmodium falciparum transportin. *Parasitology Research*, *88*(5), 391–394. https://doi.org/10.1007/s00436-001-0578-z

Yam, X. Y., Birago, C., Fratini, F., Di Girolamo, F., Raggi, C., Sargiacomo, M., Bachi, A., Berry, L., Fall, G., Currà, C., Pizzi, E., Breton, C. B., & Ponzi, M. (2013). Proteomic Analysis of Detergent-resistant Membrane Microdomains in Trophozoite Blood Stage of the Human Malaria Parasite Plasmodium falciparum. *Molecular & Cellular Proteomics*, *12*(12), 3948–3961. https://doi.org/10.1074/mcp.M113.029272

Zhang, Y. (2005). TM-align: a protein structure alignment algorithm based on the TM-score. *Nucleic Acids Research*, *33*(7), 2302–2309. https://doi.org/10.1093/nar/gki524

Zuegge, J., Ralph, S., Schmuker, M., McFadden, G. I., & Schneider, G. (2001). Deciphering apicoplast targeting signals – feature extraction from nuclear-encoded precursors of Plasmodium falciparum apicoplast proteins. *Gene*, *280*(1–2), 19–26. https://doi.org/10.1016/S0378-1119(01)00776-4

518 Figure 1

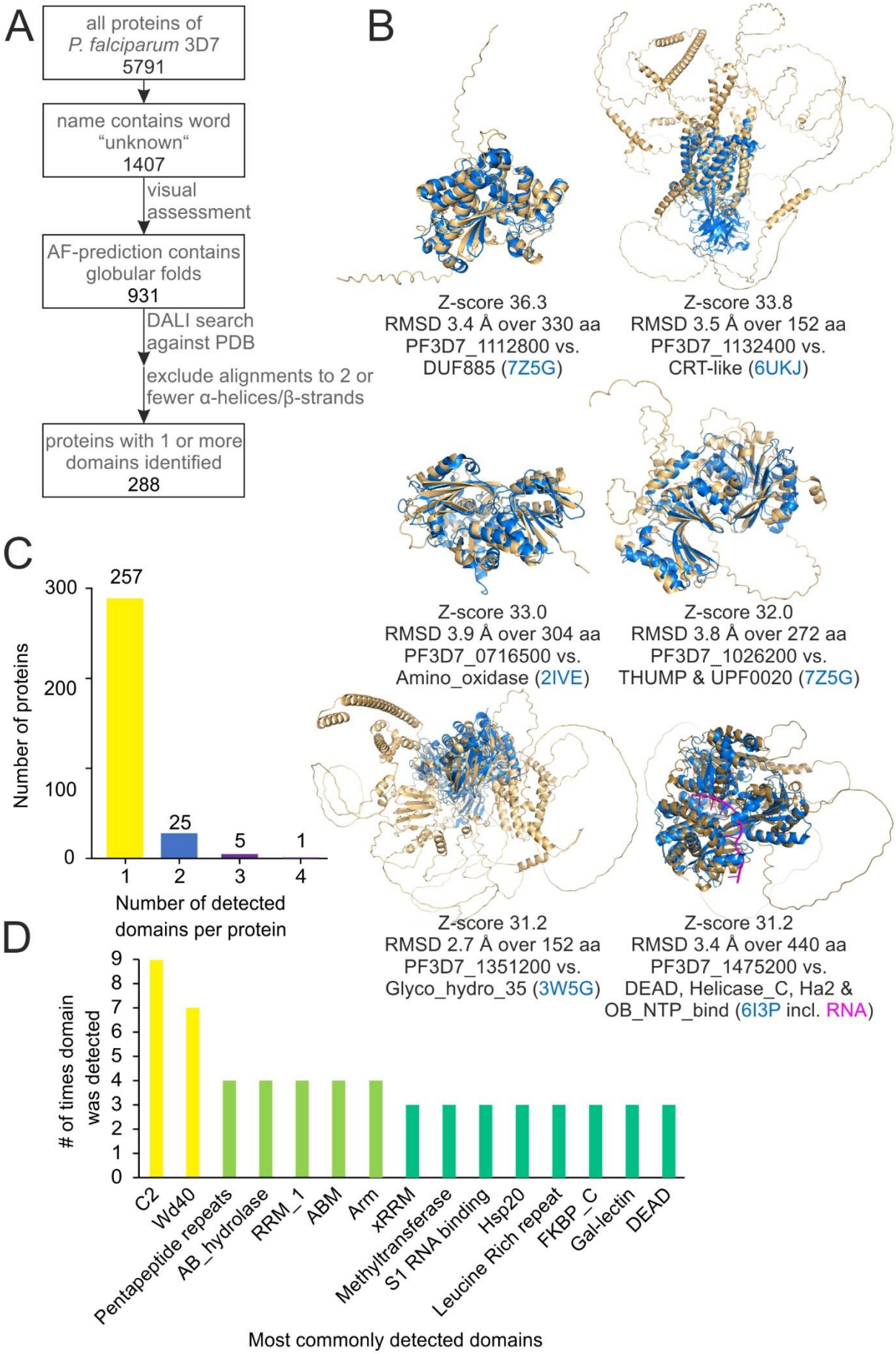

519

520 **Figure 1: Identification of domains based on similarity of Alphafold prediction to PDB structures.**
521 (A) Pipeline for detection of domains in proteins of unknown function. (B) Alignment of Alphafold
522 prediction (beige) to experimentally determined structured (blue) with domain annotation, with Z-
523 scores >30. Indicated are the Z-score resulting from the DALI search, the root mean square deviation
524 (RMSD) generated by Pymol cealign, the PlasmoDB gene accession number of the gene encoding the
525 *P. falciparum* protein, the name(s) of the domain(s) in the experimentally determined structure
526 according to Pfam and the PDB accession (blue) of the experimentally determined structure. (C)
527 Number of proteins in which one, two, three or four domains were detected by the open-ended
528 search. (D) Most commonly detected domains shown with number of times they were detected.
529 Domain names as they appear in Pfam.
530

Figure 2

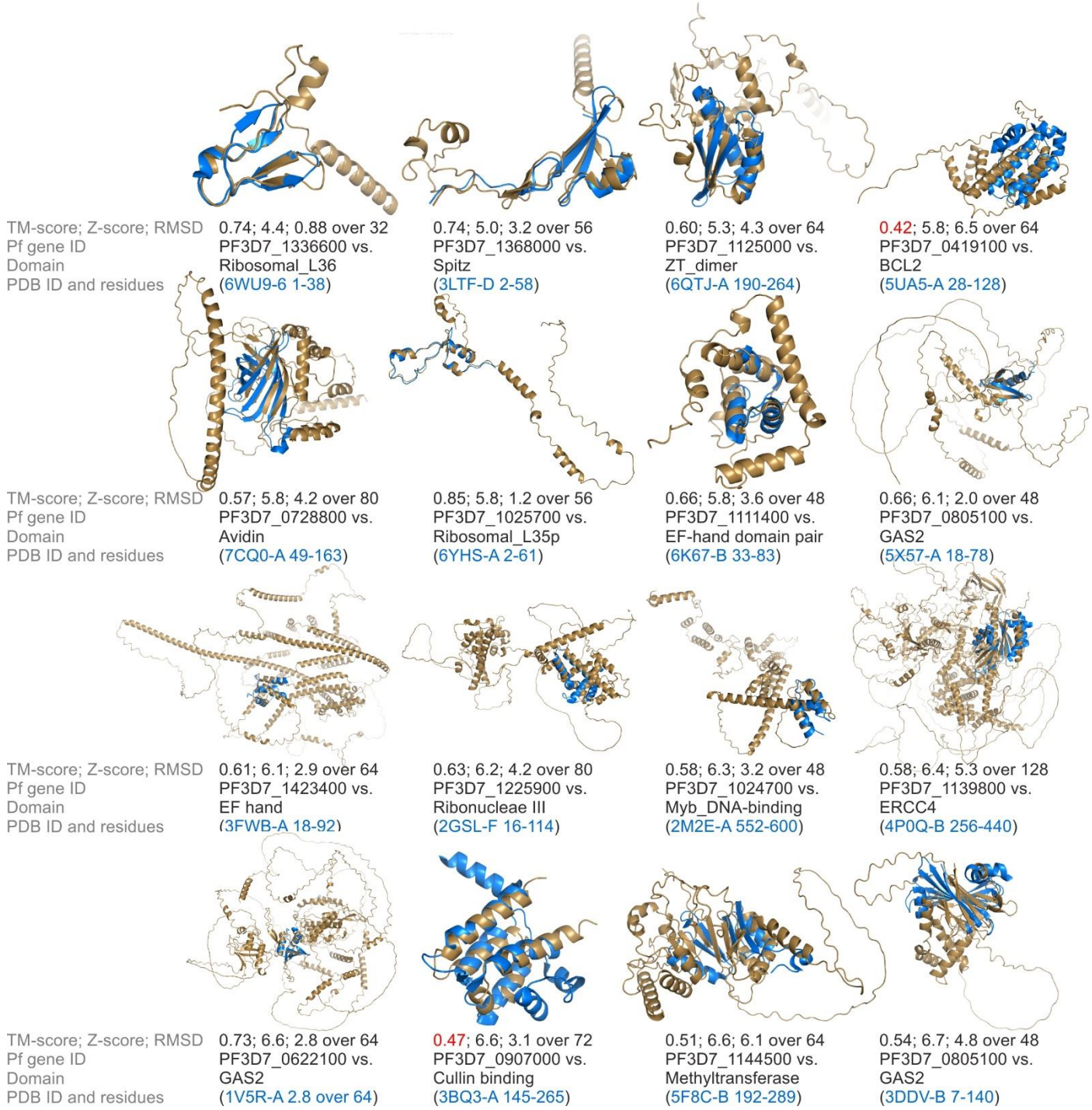

Figure 2: TM-align assessment of lowest-scoring 5% of aligned domains. The Alphafold structure of the *P. falciparum* protein (beige) is aligned to the indicated residues of the PDB structure (blue), which corresponds to the annotated domain. Given are TM-score generated by TM-align, Z-score generated by DALI, RMSD generated by Pymol cealign, PlasmoDB gene ID of *P. falciparum* gene that encodes the respective protein, name of the identified domain of similarity, the PDB ID of the structure that contained the domain and the amino acid residues at which the domain was found. For 3FWB-A residues 18 to 92 are shown even though the annotated domain only including residues 24-52 because structural similarity extended to this region. TM-scores under 0.5 are shown in red.

542 Figure 3

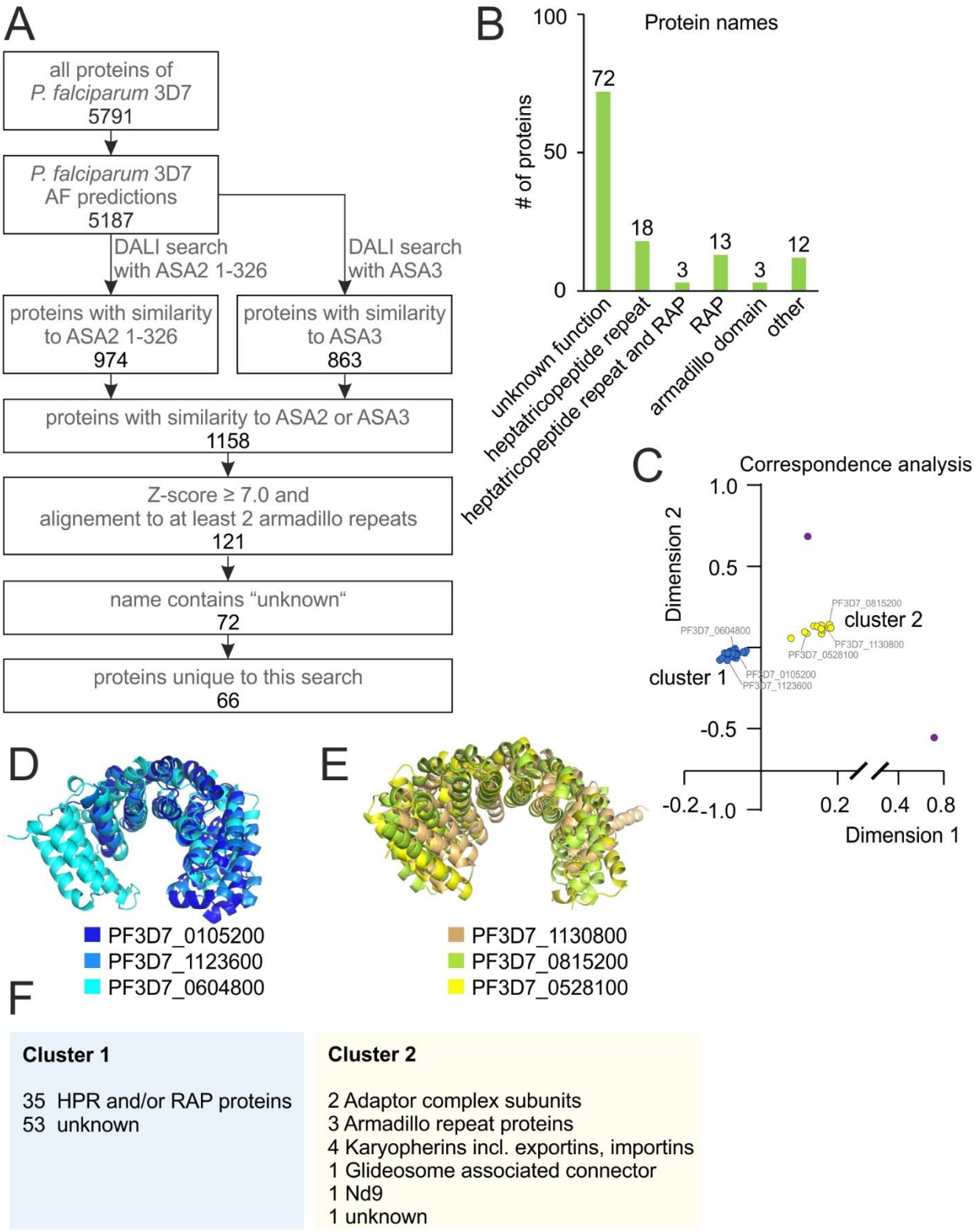

543

544 **Figure 3: Identification of ASA2/3-like armadillo domains in *P. falciparum* proteins using Alphafold**
545 **predictions.** (A) Pipeline for detection of ASA2/3-like armadillo domains. (B) Annotations of *P.*
546 *falciparum* proteins which were found to be similar to ASA2 and ASA3. (C) Correspondence analysis
547 to cluster annotated *P. falciparum* proteins with similarity to ASA2 and ASA3 by structural similarity
548 to each other. Dots corresponding to proteins shown in (D) and (E) are labelled. Purple dots do not
549 belong to cluster 1 or 2. (D) Three representative structures selected from cluster 1 as defined in (C)

550 aligned to each other using cealign in Pymol. (E) Three representative structures selected from
551 cluster 2 as defined in (C). Structures shown in (D) and (E) were used to sort *P. falciparum* proteins of
552 unknown function with similarity to ASA2 and ASA3 into clusters 1 and 2. (F) Number of proteins of
553 different functions in cluster 1 and 2.
554

555 Supplementary Figure 1

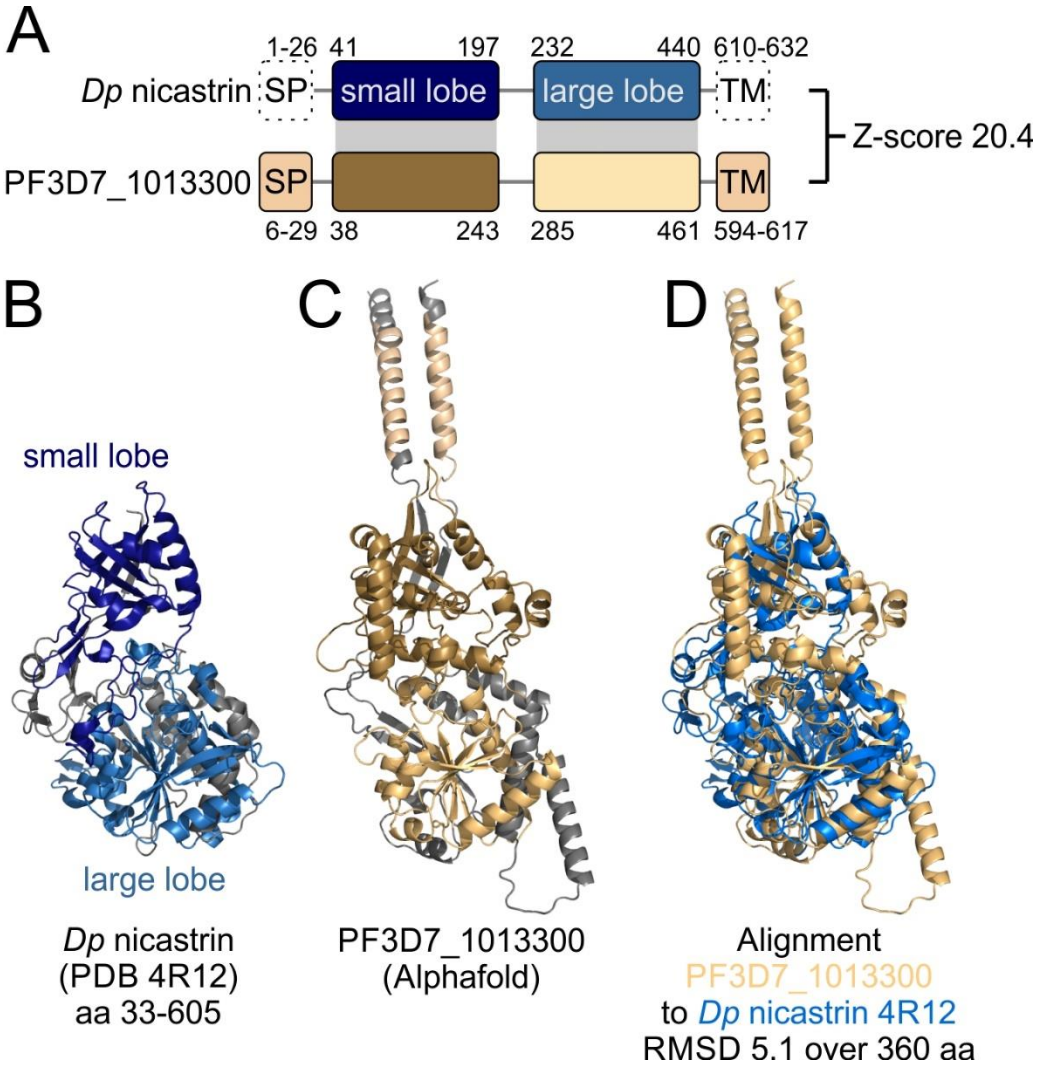

556
557

558 **Supplementary Figure 1: Nicastrin domains detected in PF3D7_1013300.** (A) Schematic
559 representation of *Dictyostelium purpureum* nicastrin and PF3D7_1013300 (not to scale). Grey
560 elements show corresponding domains. Z-score resulting from DALI score is indicated. Secondary
561 structure elements of *D. purpureum* nicastrin that are not present in the crystal structure PDB 4R12
562 are shown with dashed lines. SP, predicted signal peptide; TM, transmembrane domain. (B) Crystal
563 structure of *D. purpureum* nicastrin (PDB 4R12). Residues coloured as in (A). (C) Alphfold structure
564 prediction of PF3D7_1013300. Residues coloured as in (A). (D) *D. purpureum* nicastrin (PDB 4R12,
565 blue) and Alphfold structure prediction of PF3D7_1013300 (beige) aligned to each other using cealign
566 in Pymol. RMSD generated by Pymol cealign is indicated.
567

568 Supplementary Figure 2

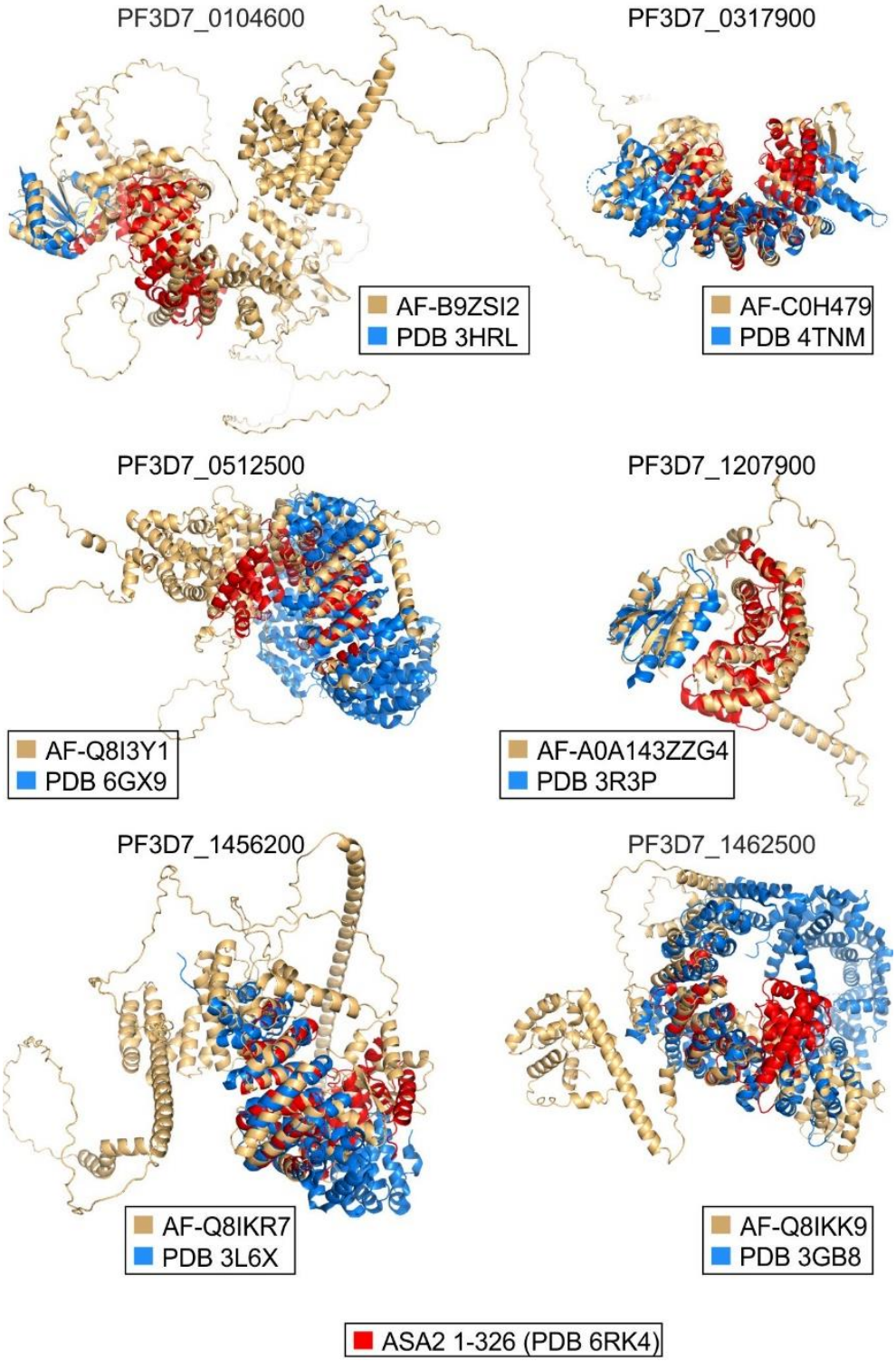

569

570 **Supplementary Figure 2: Spatial overlap of ASA2 with hits identified in open-ended domain search.**
571 Alphafold structure predictions of proteins for which domains were found in the open-ended search
572 and in the ASA2/ASA3-based search are shown (beige), and aligned to ASA2 residues 1-326 from PDB
573 6RK4 (red) and to the highest-scoring domain-annotated hit of the open-ended search (blue). For
574 PF3D7_1207900 only ASA2 residues 1-170 are shown for clarity. For PF3D7_0104600 and
575 PF3D7_1207900 the domains from the open-ended search (both DUF559, blue) and the armadillo
576 domain (red) align to different regions of the target protein. For the other four structures the
577 domains align to the same region of the target protein.

578 Supplementary Figure 3

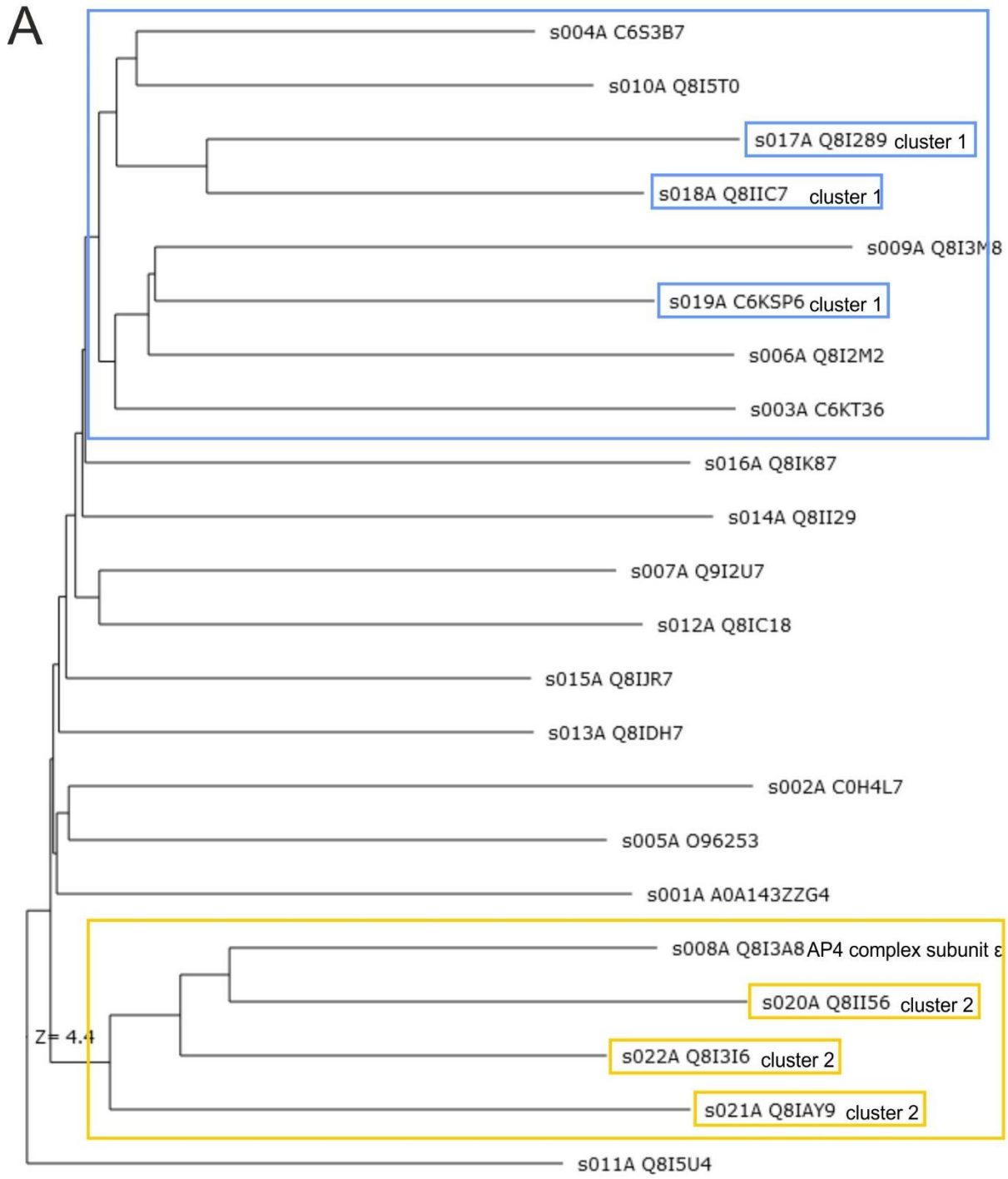

579

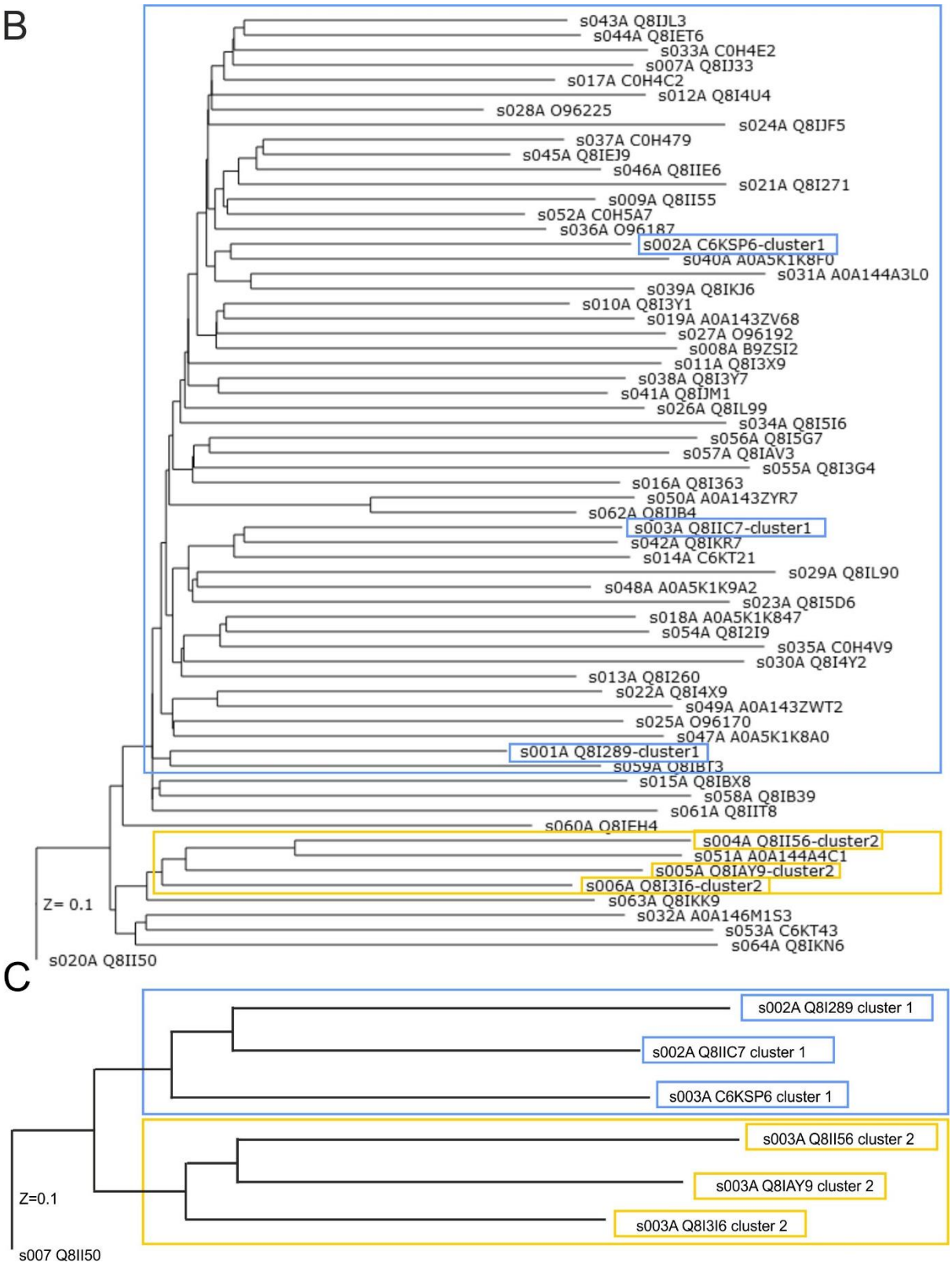

Supplementary Figure 3: Structure based clustering of unknown proteins with ASA2/ASA3-like armadillo domains by DALI all-against-all search. Proteins of known functions which are representative of cluster 1 are labelled and highlighted in blue, those representative of cluster 2 are labelled and highlighted in yellow. Proteins considered to belong to the same cluster as the representative proteins are framed in the same color. (A) Batch 1. (B) Batch 2. (C) Batch 3.